21st European Workshop on White Dwarfs
Castanheira, Campos, Montgomery, eds.
July 23–27, 2018, Austin, Texas, USA

An Exploration of Spotted White Dwarfs from K2

Joshua S. Reding[1], JJ Hermes[1,2], J. Christopher Clemens[1]

[1] *University of North Carolina at Chapel Hill, Chapel Hill, NC, USA;*
jsreding@unc.edu, jjhermes@unc.edu, clemens@physics.unc.edu
[2] *Hubble Fellow*

Abstract

The Kepler K2 mission has discovered a significant population of white dwarf stars that exhibit photometric variability due to surface inhomogeneities likely related to magnetism. These "spotted" white dwarfs present not only in temperature regimes where we expect convection to dominate white dwarf photospheres, but also where radiation should dominate. We present an exploration of spotted white dwarfs as a function of various physical characteristics, including temperature, magnetic field strength, and rotational period, in order to better understand the origins of these photometric variations.

1 Introduction

White dwarfs which present photometric variability due to surface spots have been individually investigated in a number of cases (Brinkworth et al., 2005; Holberg & Howell, 2011; Kilic et al., 2015). These objects most commonly present with kG to MG magnetic fields, and surface temperatures less than $10,000K$, suggesting dark spot formation due to local suppression of atmospheric convection from magnetism. However, as discussed by Maoz et al. (2015), some objects have been observed which exhibit similar variability, but must have radiative atmospheres as suggested by their measured effective temperatures ($T_{\rm eff} > 12,000-14,000K$). There are a number of potential explanations, including ultraviolet absorption due to atmospheric metals which is re-emitted in the optical, or ongoing material accretion to the white dwarf surface (Maoz et al., 2015; Hallakoun et al., 2018). Both of these phenomena are facilitated by the presence of a strong magnetic field, which will constrain accretion or optical re-emission to small regions, making them appear as surface "bright" spots. For both types of spot incidence, we observe variability periods on the order of days to fractions of a day, which is consistent with asteroseismically measured rotation periods (Hermes et al., 2017a).

Given that both types of spot incidence involve magnetism, the two may likely share a similar origin related to the presence of a strong magnetic field in the star. Nordhaus et al. (2011) suggest that white dwarf magnetism may be induced when the star is still in its giant stage, and accretes material or a smaller body via common envelope interaction. Another explanation from García-Berro et al. (2012) proposes that magnetism can be induced in double degenerate mergers. These two possibilities mirror the single- and double-degenerate progenitor scenarios for type-Ia supernovae, and so exploration of spotted magnetic white dwarfs is relevant in addressing the type-Ia progenitor question.

As of the *K2* mission's Campaign 16, the *Kepler* Space Telescope has observed over 2000 white dwarfs, white dwarf candidates, and similar objects along the ecliptic plane (`k2wd.org`). This data is an unparalleled resource for exploring white dwarf variability both for its quality and for the quantity of observations taken. Hallakoun et al. (2018) explore the *Kepler* sample in the context of possible debris accretion, while Maoz et al. (2015) and Hermes et al. (2017b) discuss particular examples which likely present variation due to surface spots. Here, in order to holistically evaluate spotted white dwarfs as a class, we explore broad characteristics exhibited by the population observed by *Kepler*.

2 Selection Criteria

Given the large catalogue of white dwarf candidates observed by *Kepler*, our first task was to identify objects whose variability is caused by surface spots. However, because there is no direct way of confirming that spots are the cause of observed variability, our method was to instead rule out other potential sources.

The first potential contaminating mechanism we considered was binarity, in which photometric variation is driven by the reflection of a hot white dwarf off the surface of a larger and cooler companion, such as a main sequence star. The variability is therefore a consequence of the orbital period of the binary system. We can confirm whether a white dwarf is in a reflec-

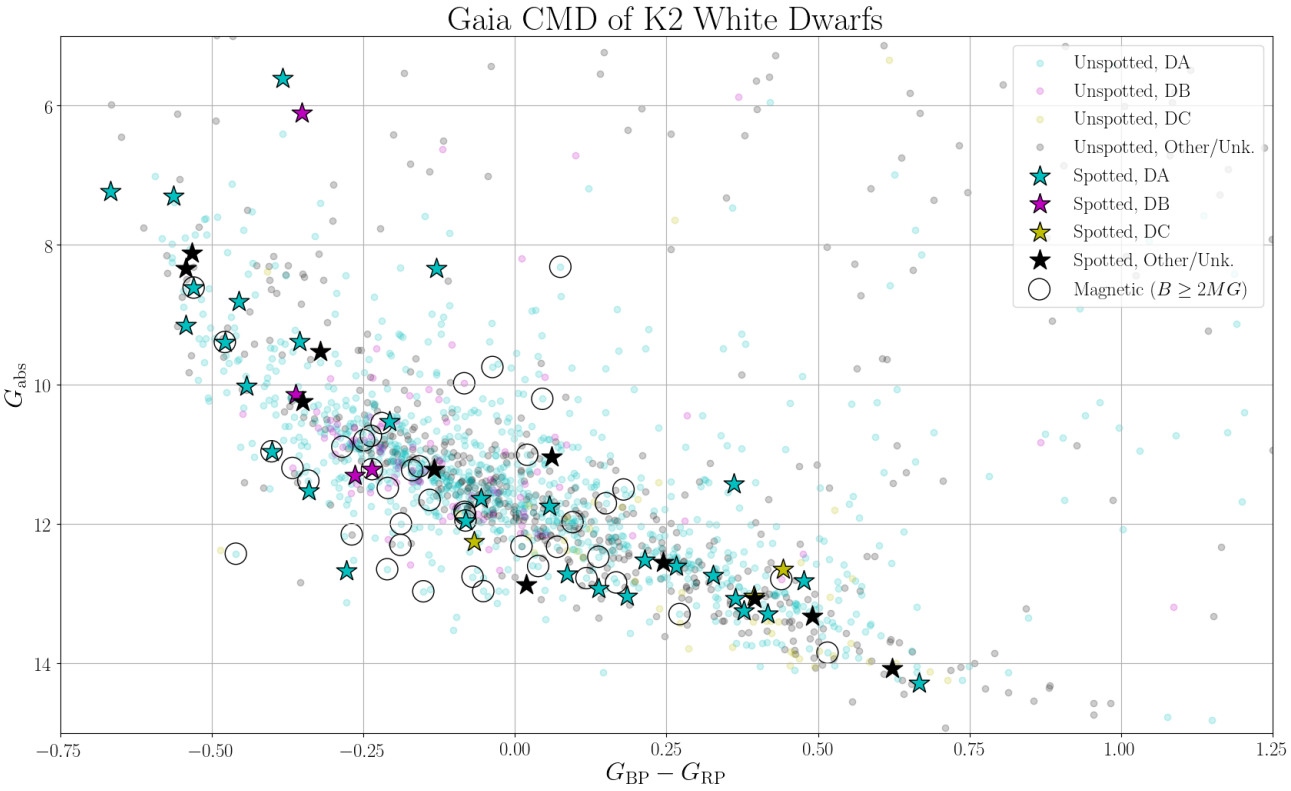

Figure 1: *Gaia* color-magnitude diagram of all *K2* objects. We acknowledge three DA white dwarfs and one DB which we flag as "spotted," but may be in unresolved binary systems given their CMD locations above the main white dwarf track. These require radial velocity observations to rule out binarity or Doppler beaming as a source of variability.

tion binary by inspecting its spectrum. Given the high temperature of the white dwarf, its spectrum would be strongly blue, while the companion would present as an excess at redder wavelengths. This is confirmed by fitting standard white dwarf models to the spectrum peak below $\sim$ 7000 Å, and then evaluating the fit at longer wavelengths, along with possible presentation of features unique to a main sequence companion such as Na I $\lambda\lambda$ absorption at $\sim$ 8190 Å, and Hα emission (Rebassa-Mansergas et al., 2007). We exclude these from our analysis by cross-referencing our sample with the full *SDSS* WD-MS catalogue.

As a final check that we have excluded binaries, we produced a *Gaia* color-magnitude diagram of *Kepler* objects to find photometric excesses which may be caused by a companion (Figure 1). From this, it appears that four objects we have flagged as "spotted" may in fact be in unresolved binaries based on their positions above most of the white dwarf track. We will follow up these objects with future spectral observations to measure possible radial velocity shifts. These measurements would also allow us to rule out Doppler beaming from orbital motion as a potential source of variability (Zucker et al., 2007).

The second potential contaminating mechanism is pulsation. Both hydrogen- (DA) and helium-atmosphere (DB) white dwarfs are known to pulsate within specific temperature ranges, known as "instability strips." These are located at $\sim 10,500 - 12,500K$ for DA white dwarfs, and $\sim 20,000 - 32,000K$ for DB (Winget & Kepler, 2008). However, like longer periods for binarity, this again is not a definitive means of categorizing variability as being due to pulsations. We gain a second clue by inspecting the Fourier transform of the object data, as pulsations are typically quite short in period (100s of seconds), and often have asymmetric periodogram spacings. They also may exhibit splitting in individual periodogram peaks, which can be used to measure rotation rates (Hermes et al., 2017a).

Applying these criteria to the *Kepler* sample left us with 57 white dwarfs which present variability we attribute to spot modulation. In order to place these within the context of the whole white dwarf sample, we investigated relevant physical characteristics, including $\log g$ and $T_{\rm eff}$, rotational period, and magnetism (from previously published work).

3 Data & Methodology

In order to evaluate the spotted population in the context of the whole *Kepler* white dwarf catalogue, we sought to build as large a sample as possible of $\log g$

and $T_{\rm eff}$ values for *Kepler* white dwarfs. As of Campaign 16, 1090 of the $2000+$ objects have $\log g$ and $T_{\rm eff}$ from previous spectroscopy. These values were collected from various published sources (mostly *SDSS*), or computed from our own observations using the Goodman High-Throughput Spectrograph on the SOuthern Astrophysical Research (*SOAR*) 4.1m Telescope on Cerro Pachon, Chile. Our typical setup for white dwarf spectral typing and parameter estimation gives us a wavelength coverage of approximately $3800 - 5400$Å, which contains the higher-order Balmer features, at a resolving power of $R \approx 4450$. We also have a field estimate for a strongly magnetic spotted white dwarf from *SOAR* spectra, discussed in Section 4.3.

While most of the *Kepler* objects had previous $\log g$ and $T_{\rm eff}$ from spectroscopy, in order to make our sample as complete as possible, we used *SDSS* photometry and the Bergeron DA cooling models (Holberg & Bergeron, 2006; Kowalski & Saumon, 2006; Tremblay et al., 2011; Bergeron et al., 2011) to produce rough parameter estimates where there were not previous spectral values. We interpolated the models bicubically into $u-g, g-r$ color space, and then for a given object with *SDSS* photometry, we extracted the model $\log g$ and $T_{\rm eff}$ contours which intersected at the appropriate color index values. This method provided us with 342 additional estimates, bringing our total sample size for analysis to 1432 white dwarfs. These constraints also limit our sample of 57 spotted white dwarfs to 44 with parameter solutions. This gives our measurable population a spot incidence rate of $\sim 3\%$, which is consistent with the magnetism incidence rate for *SDSS* white dwarfs of $\sim 4\%$ given in Kepler et al. (2013).

To analyze variability, we retrieved individual light curves for our objects from the *Kepler K2* archive. For each campaign in the *K2* mission, *Kepler* observed the field for ~ 80 days at either a long-cadence sampling rate of every 30 minutes, or a short-cadence rate of every 1 minute. For both types of datasets, this allowed us to analyze light curves with thousands of data points, thereby granting us excellent constraints on variability periods and amplitudes.

We computed Lomb-Scargle periodograms from the *Kepler* light curves using the `astropy.stats` Python package, setting a maximum period cutoff of 10 days, above which the *K2* field observation duration makes period identification difficult. Additionally, in our periodograms we masked out integer harmonics of $47.2042 \mu Hz$, as these result from the *K2* drift correction thruster firing every 5.9 hours. We applied a significance threshold of 5 times the average value of the periodogram to choose peaks likely associated with spots for investigation, and performed a least squares fit to the light curve data (using these peak locations as an initial guess) in order to find the most accurate rotation period. Finally, we visually inspected the light curves folded on these periods for a regular structure indicative of spot profiles. Some examples of folded curves are presented in Section 4.3.

4 Results

4.1 $\log g$ and $T_{\rm eff}$

Our collected $\log g$ and $T_{\rm eff}$ plot of *Kepler* objects is presented in Figure 2. The first apparent result from this plot is that spotted white dwarfs appear to cluster in the extreme temperature ranges of $<\sim 10kK$ and $>\sim 29kK$, while very few fall between, despite this range being where the great majority of the unspotted sample lies (Table 1). We therefore recommend searching in these extreme regimes for future discovery of spotted white dwarfs.

This dichotomy is especially interesting when put in the context of white dwarf atmospheric physics, as the cooler regime encompasses where we expect atmospheres to be convective, while atmospheres in the hotter regime should be radiative. It makes intuitive sense that we observe spots on white dwarfs with convective atmospheres, as the mechanism by which those spots form may be similar to that by which sunspots are formed, i.e. by magnetic fields locally suppressing convection. In contrast, it is not immediately apparent how we can see spots in radiative atmospheres, though our findings described in Section 4.3 may offer a clue. We defer discussion to that section of the paper.

Table 1: Distribution of spotted white dwarfs within *Kepler* sample, separated by regions of interest.

Approx. $T_{\rm eff}$	$< 10kK$	$10kK - 29kK$	$> 29kK$
Total WDs	400	900	132
Spotted	17	10	17
% Spotted	$\mathbf{4.25\%}$	$\mathbf{1.1\%}$	$\mathbf{12.9\%}$

4.2 Rotational Periods

Hermes et al. (2017a) discusses how *Kepler* data can be used to measure rotational periods via splitting of periodogram peaks associated with pulsation. In Figure 3, we plot our distribution of rotational periods from spot modulation, along with the distribution of rotational periods measured from asteroseismology. We note similar peak locations in our distribution as compared to asteroseismology, which strongly suggests that spot variability indeed occurs at a period set by stellar rotation. However, the spotted distribution shows a significant tail approaching extremely short periods, on the order of minutes.

We note that 3 objects in this short-period tail are hot DQV (variable, carbon-atmosphere) white dwarfs. This

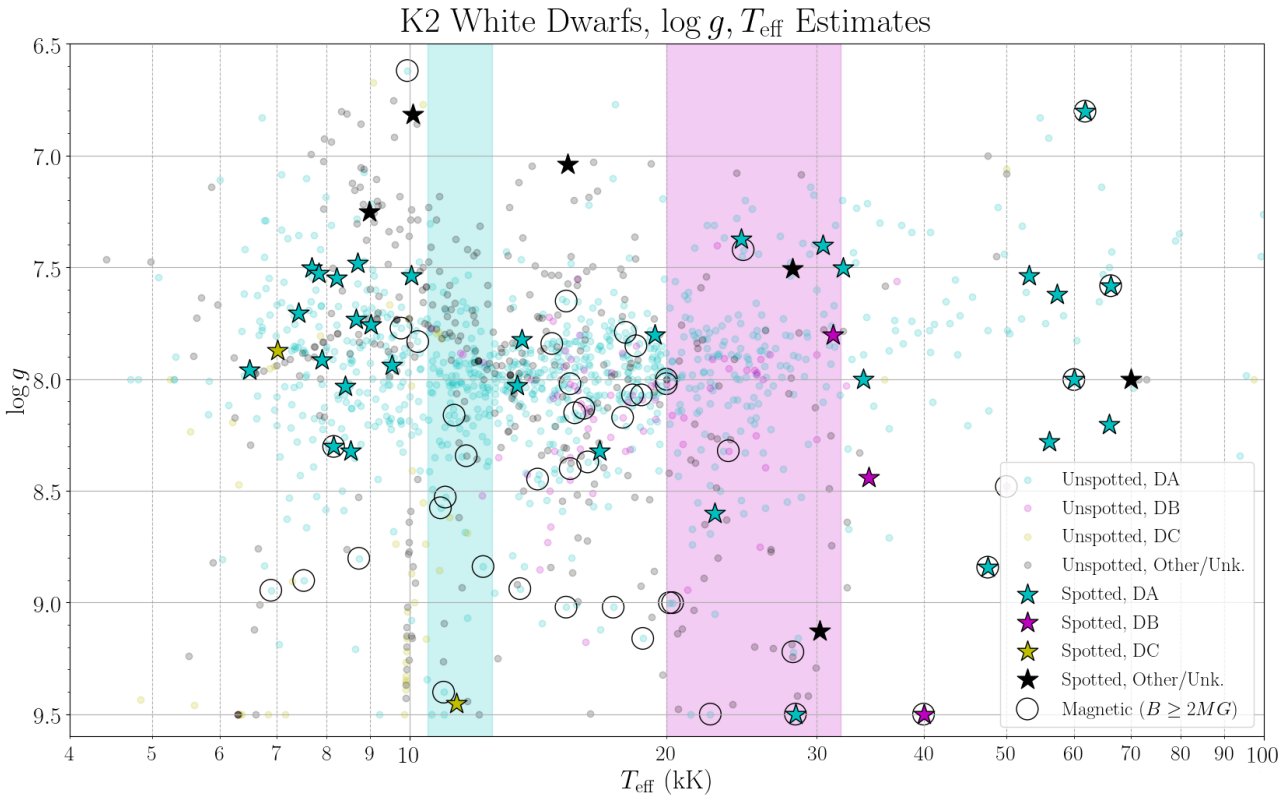

Figure 2: Collected $T_{\rm eff}$ and $\log g$ estimates for K2 white dwarfs. We highlight the DA and DB instability strips according to their respective legend colors, and mark incidences of "strong" magnetism using a lower threshold of $2MG$ (Kleinman et al., 2013; Kepler et al., 2016). There are apparent overdensities of spotted white dwarfs below $\sim 10,000K$ and above $\sim 30,000K$, but fewer between, where the vast majority of white dwarfs lie.

relatively new class of white dwarf has been identified as presenting short singular-period modulation and strong magnetism (Williams et al., 2016). Our finding that DQVs produce this significant section of short-period outliers in the distribution offers support to the theory that DQV white dwarfs may result from spun-up double degenerate mergers, and therefore may be evidence of a failed type-Ia supernovae (Dunlap & Clemens, 2015).

4.3 Magnetism

Magnetism in white dwarf stars has been explored both broadly in surveys and in detail for individual objects, and with varying thresholds of detection. Therefore, in order to investigate magnetism fairly for the spotted *Kepler* sample, we chose a lower field strength limit of $2MG$ to flag something as "strongly" magnetic. This is the same limit applied by Kleinman et al. (2013) and Kepler et al. (2016) in their respective *SDSS* data release publications to classify a new white dwarf as magnetic. We would like to note, however, that a "strong" field is not necessary to associate magnetism with spot formation. Figure 4 illustrates this via a spotted DA white dwarf with a complex folded light curve, yet a relatively weak magnetic field of $350kG$ (Holberg & Howell, 2011). We also note that spotted white dwarfs with detected magnetic splitting seem to exhibit the

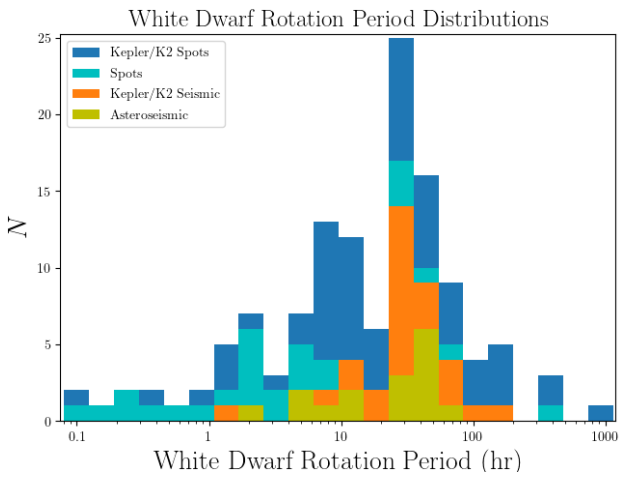

Figure 3: Period distributions (stacked) for rotating white dwarfs as measured from spot modulation and asteroseismology (Kawaler, 2015; Hermes et al., 2017a). We note a significant tail approaching extremely short periods for spotted objects, and which includes 3 DQV white dwarfs.

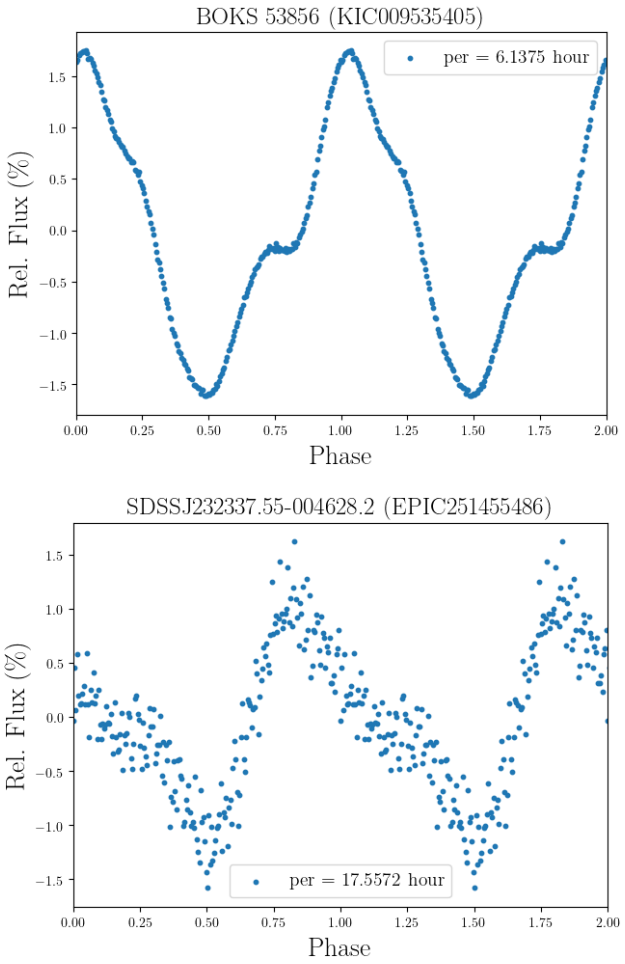

Figure 4: Two folded *K2* light curves of confirmed magnetic white dwarfs. The top is a DA white dwarf (DAH; $T_{\rm eff} = 34,000, \log g = 8.0$) with a measured field strength of $350kG$ (Holberg & Howell, 2011), while the bottom (DBH; $T_{\rm eff} = 40,000, \log g = 9.5$) has a $4.8MG$ field (Schmidt et al., 2003). This illustrates that even weak magnetic fields may be associated with spot formation.

most non-sinusoidal folded light curves, as shown in Figures 4 and 5. The plots are folded such that the variability minimum occurs at a phase of 0.5.

Our most interesting result regarding magnetism is that of the 7 strongly magnetic spotted white dwarfs from *Kepler*, 6 of them have $T_{\rm eff}$ in the aforementioned high-temperature radiative regime. This suggests that magnetism significantly contributes to the appearance of spots in white dwarfs with radiative atmospheres. Fendt & Dravins (2000) offer a potential explanation for this phenomenon, in which magnetic fields can lower the scale height of white dwarf atmospheres, revealing hotter material below and producing photometrically-detectable bright spots.

The only strongly magnetic white dwarf in the *Kepler* sample which falls in the convective regime is shown in Figure 5. This object was measured using *SOAR* to have a $2.4MG$ magnetic field (M. Hollands, private communication), and exhibits the most complex folded light curve we've yet found in a *Kepler* spotted white dwarf. This light curve shape is dominated by a high-order, likely octupole, magnetic field topology (S. Kawaler, private communication), in which there are four spots in mirrored pairs on opposite sides of the star. This presents four peaks per phase, with peak height dependent on inclination of the white dwarf's rotation axis relative to our line of sight. This object offers a promising indication that stronger magnetic activity may significantly affect the surfaces of white dwarfs with convective atmospheres, suppressing convection in multiple locations according to the topology of the field, and therefore can produce complex spot profiles.

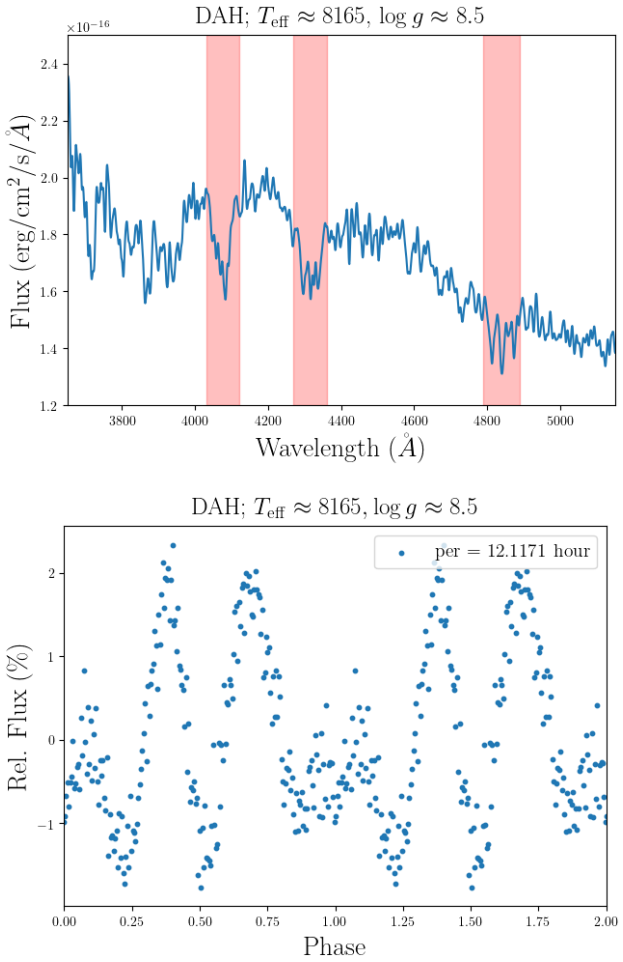

Figure 5: Top: *SOAR* spectrum and bottom: folded light curve for a white dwarf with a high-order spot profile, as shown from the odd shape containing four peaks per phase. We mark Zeeman splitting in $H\beta$, $H\gamma$, and $H\delta$ in the spectrum. This object is also notable as the only strongly magnetic ($B = 2.4MG$) *Kepler* white dwarf in the $< 10,000K$ temperature range.

5 Conclusions

We present a holistic analysis of *Kepler* space telescope spotted white dwarfs via the physical parameters of $\log g$ and $T_{\rm eff}$, rotational period, and magnetic field. We perform our analysis on 44 white dwarfs which exhibit variability due to spot modulation, amongst a total population of 1432 white dwarfs observed by *Kepler*. Of these 1432 stars, 1090 have measurements of $\log g$ and $T_{\rm eff}$ from spectroscopy, and 342 have estimates from fitting *SDSS* photometry to the Bergeron DA white dwarf cooling models.

We find that spotted white dwarfs preferentially cluster in extreme temperature regimes of $<\sim 10kK$ and $>\sim 29kK$, in contrast to the vast majority of unspotted white dwarfs, which fall between these limits (Table 1). We expect cooler white dwarfs to exhibit convective atmospheres, which may contribute to spot formation, while hotter ones should exhibit radiative atmospheres. Magnetism seems a likely contributor to spot formation in this hotter regime, and in the cooler regime it may suppress convection in multiple locations according to the star's magnetic field topology, producing complex spot profiles.

We compare the distribution of rotational periods measured via spots to that as measured via asteroseismology. These two profiles cover similar period ranges, but the spotted distribution presents a significant tail approaching very short periods, on the order of minutes. Much of this short-period tail is composed of DQV white dwarfs, which suggests that this class of star may result from double degenerate mergers which had insufficient conditions to produce a type-Ia supernova detonation.

Lastly, we apply a lower limit to field strength of $2MG$ to classify an object as "strongly" magnetic. 6 of the 7 strongly magnetic spotted white dwarfs in our sample have $T_{\rm eff}$ in our high-temperature regime, while the one in the lower regime presents a complex spot profile which can be replicated by a high-order field topology. We also show that "strong" magnetism is not necessarily required to produce spots, and so spots are potentially broadly associated with magnetism.

Acknowledgements. Support for this work was provided by NASA through Hubble Fellowship grant #HST-HF2-51357.001-A, awarded by the Space Telescope Science Institute, which is operated by the Association of Universities for Research in Astronomy, Incorporated, under NASA contract NAS5-26555, as well as NASA *K2* Cycle 4 Grant NNX17AE92G. Based on observations obtained at the Southern Astrophysical Research (SOAR) telescope, which is a joint project of the Ministério da Ciência, Tecnologia, e Inovação da República Federativa do Brasil, the U.S. National Optical Astronomy Observatory, the University of North Carolina at Chapel Hill, and Michigan State University.

References

Bergeron P., et al., 2011, ApJ, 737, 28

Brinkworth C. S., Marsh T. R., Morales-Rueda L., Maxted P. F. L., Burleigh M. R., Good S. A., 2005, MNRAS, 357, 333

Dunlap B. H., Clemens J. C., 2015, in Dufour P., Bergeron P., Fontaine G., eds, Astronomical Society of the Pacific Conference Series Vol. 493, 19th European Workshop on White Dwarfs. p. 547

Fendt C., Dravins D., 2000, Astronomische Nachrichten, 321, 193

García-Berro E., et al., 2012, ApJ, 749, 25

Hallakoun N., et al., 2018, MNRAS, 476, 933

Hermes J. J., et al., 2017a, ApJS, 232, 23

Hermes J. J., Gänsicke B. T., Gentile Fusillo N. P., Raddi R., Hollands M. A., Dennihy E., Fuchs J. T., Redfield S., 2017b, MNRAS, 468, 1946

Holberg J. B., Bergeron P., 2006, AJ, 132, 1221

Holberg J. B., Howell S. B., 2011, AJ, 142, 62

Kawaler S. D., 2015, in Dufour P., Bergeron P., Fontaine G., eds, Astronomical Society of the Pacific Conference Series Vol. 493, 19th European Workshop on White Dwarfs. p. 65 (arXiv:1410.6934)

Kepler S. O., et al., 2013, MNRAS, 429, 2934

Kepler S. O., et al., 2016, MNRAS, 455, 3413

Kilic M., et al., 2015, ApJ, 814, L31

Kleinman S. J., et al., 2013, ApJS, 204, 5

Kowalski P. M., Saumon D., 2006, ApJ, 651, L137

Maoz D., Mazeh T., McQuillan A., 2015, MNRAS, 447, 1749

Nordhaus J., Wellons S., Spiegel D. S., Metzger B. D., Blackman E. G., 2011, Proceedings of the National Academy of Science, 108, 3135

Rebassa-Mansergas A., Gänsicke B. T., Rodríguez-Gil P., Schreiber M. R., Koester D., 2007, MNRAS, 382, 1377

Schmidt G. D., et al., 2003, ApJ, 595, 1101

Tremblay P.-E., Bergeron P., Gianninas A., 2011, ApJ, 730, 128

Williams K. A., Montgomery M. H., Winget D. E., Falcon R. E., Bierwagen M., 2016, ApJ, 817, 27

Winget D. E., Kepler S. O., 2008, ARA&A, 46, 157

Zucker S., Mazeh T., Alexander T., 2007, ApJ, 670, 1326